MEMORY TRICKS: IMPROVING ACTIVE INTERFERENCE CANCELLATION FOR OUT-OF-BAND POWER REDUCTION IN OFDM

Khawar Hussain *Roberto López-Valcarce*

atlanTTic Research Center, Universidade de Vigo, Vigo, Spain

ABSTRACT

Although active interference cancellation (AIC) is an appealing approach to reduce out-of-band radiation (OBR) in multicarrier systems without distorting data subcarriers, it usually requires a large number of reserved subcarriers to be effective. Introducing memory in AIC precoding may help alleviate this drawback in exchange for some increase in computational complexity. We propose a novel memory AIC precoder which, in contrast to previous schemes, minimizes OBR within a user-selectable frequency region and allows for controlling spectral overshoot.

Index Terms— OFDM, out-of-band radiation, sidelobe suppression, spectrum shaping, spectral precoding.

1. INTRODUCTION

Orthogonal frequency division multiplexing (OFDM) has been chosen for the 5G New Radio (5G-NR) interface by the Third Generation Partnership Project (3GPP) [1]. OFDM is a mature multicarrier modulation scheme with many advantages: it is spectrally efficient, robust against frequency-selective channels, and well matched to multiple input-multiple output operation. Nonetheless, it suffers from large spectrum sidelobes, causing high out-of-band radiation (OBR) and large levels of adjacent channel interference. The OBR problem has been traditionally addressed with a variety of techniques. Established methods such as guard band insertion, filtering [2], or windowing (pulse shaping) [3, 4] are simple and straightforward, but they either degrade spectral efficiency or reduce the effective cyclic prefix (CP) length.

Another approach to reduce OBR is spectral precoding [5–8], by which the transmitted symbols are obtained by some transformation of the original data sequence. In general, precoding distorts the data, so that appropriate decoding must be applied at the receiver to avoid error rate degradation. In some applications this approach is not feasible, e.g., according to the 3GPP NR specification [1], any operation performed on CP-OFDM at the transmitter side must be receiver agnostic [9]. Active interference cancellation (AIC) [10, 11] can be regarded as a particular case of precoding, in which a subset of subcarriers (termed *cancellation subcarriers*) is reserved for OBR reduction, whereas the data subcarriers are not modified. In this way, the receiver can simply discard the cancellation subcarriers, and no decoding is needed. Thus, AIC is completely transparent to the receiver [12, 13]. Because the constraint that data subcarriers remain unaltered results in lower OBR reduction with respect to general precoders allowing some data distortion, it is of interest to investigate improved AIC schemes with better OBR performance.

AIC techniques usually modulate the cancellation subcarriers by some linear combination of the values transmitted in the data subcarriers of the *same* OFDM symbol [14], and thus they can be referred to as *memoryless.* It is pertinent to ask whether performance could be improved by introducing memory in AIC precoding, so that the data from OFDM symbols other than the current one affects the computation of the cancellation weights. For example, the design from [15] imposes continuity of the time-domain signal and its derivatives at the transition between consecutive symbols, resulting in a memory precoder (a first-order infinite impulse response (IIR) filter applied to the data sequence) which provides good OBR performance but suffers from two drawbacks: it does not allow to give more emphasis to the effect of OBR in a particular frequency region over others; and it tends to yield large overshoot values in the power spectral density (PSD), unless a large fraction of subcarriers is reserved for cancellation purposes. A modification was proposed in [16], which constrains the power of reserved subcarriers; although this may be effective in controlling PSD overshoot, it results in significant performance loss and requires to solve an optimization problem for each OFDM symbol, which has high online complexity.

We present AIC memory precoders based on finite impulse response (FIR) filters. Based on a novel expression for the PSD under memory precoding, the proposed design minimizes OBR over a user-selectable frequency region and allows for effective control of PSD overshoot. Precoder coefficients are data-independent and can be computed offline. Simulation results illustrate the design tradeoffs involving OBR reduction, spectral efficiency, complexity, and spectral overshoot.

Supported by Agencia Estatal de Investigación (Spain) and the European Regional Development Fund (ERDF) (PID2019-105717RB-C21, BES-2017-080305), and by Xunta de Galicia (atlanTTic accreditation 2020-2023, Grupo de Referencia ED431C2017/53). Email: {khawar,valcarce}@gts.uvigo.es

2. SIGNAL MODEL

Consider a multicarrier system with IFFT size N and a guard interval of P samples. The set of indices of the $K \leq N$ active subcarriers are $\mathcal{K} = \{k_1, k_2, \cdots k_K\}$, and $x_k^{(m)} \in \mathbb{C}$ is the data modulated on the k-th subcarrier of the m-th symbol. The baseband samples of the multicarrier signal are given by

$$s[n] = \sum_{m=-\infty}^{\infty} \sum_{k \in \mathcal{K}} x_k^{(m)} h_{\mathrm{P}}[n - mL] e^{j\frac{2\pi}{N}k(n-mL)}, \quad (1)$$

with $L = N + P$ the symbol length in samples, and $h_{\mathrm{P}}[n]$ the shaping pulse with Fourier transform $H_{\mathrm{P}}(e^{j\omega}) = \sum_n h_{\mathrm{P}}[n] e^{-j\omega n}$. In standard CP-OFDM, $h_{\mathrm{P}}[n] = 1$ for $0 \leq n \leq L-1$, and zero otherwise. Letting T_s be the sampling interval, and thus $\Delta f = \frac{1}{NT_s}$ the subcarrier spacing, then the analog baseband signal is

$$s(t) = \sum_{n=-\infty}^{\infty} s[n] h_{\mathrm{I}}(t - nT_s), \quad (2)$$

with $h_{\mathrm{I}}(t)$ the impulse response of the interpolation filter in the Digital-to-Analog Converter (DAC), with transfer function $H_{\mathrm{I}}(f)$. Let us define $\phi_k(f) \triangleq H_{\mathrm{P}}^*(e^{j2\pi(f-k\Delta f)T_s})$, and

$$\boldsymbol{\phi}(f) \triangleq \begin{bmatrix} \phi_{k_1}(f) & \phi_{k_2}(f) & \cdots & \phi_{k_K}(f) \end{bmatrix}^T \in \mathbb{C}^K. \quad (3)$$

Let us introduce the vector of data symbols in the m-th block:

$$\boldsymbol{x}_m \triangleq \begin{bmatrix} x_{k_1}^{(m)} & x_{k_2}^{(m)} & \cdots & x_{k_K}^{(m)} \end{bmatrix}^T \in \mathbb{C}^K. \quad (4)$$

It is assumed that the random process $\{\boldsymbol{x}_m\}$ is zero-mean and wide-sense stationary. Then, the power spectral density (PSD) of $s(t)$ can be shown[1] to be

$$S_s(f) = \frac{|H_{\mathrm{I}}(f)|^2}{LT_s} \boldsymbol{\phi}^H(f) \boldsymbol{S}_x(Lf) \boldsymbol{\phi}(f), \quad (5)$$

where $\boldsymbol{S}_x(f) = \sum_\ell \mathbb{E}\{\boldsymbol{x}_m \boldsymbol{x}_{m-\ell}^H\} e^{-j2\pi f T_s \ell}$.

Let $\boldsymbol{d}_m \in \mathbb{C}^D$ be the data sequence to be transmitted, with $D \leq K$. We focus on linear time-invariant memory precoders, for which $\{\boldsymbol{x}_m\}$ is generated from $\{\boldsymbol{d}_m\}$ as

$$\boldsymbol{x}_m = \sum_\ell \boldsymbol{G}_\ell \boldsymbol{d}_{m-\ell} \quad (6)$$

where $\boldsymbol{G}_\ell \in \mathbb{C}^{K \times D}$. The standard memoryless precoder architecture is obtained if $\boldsymbol{G}_\ell = \boldsymbol{0}$ for $\ell \neq 0$ in (6). Assuming the data sequence is zero-mean with $\mathbb{E}\{\boldsymbol{d}_m \boldsymbol{d}_{m-\ell}^H\} = \delta_\ell \boldsymbol{I}_D$, then $\boldsymbol{S}_x(f)$ in (5) becomes $\boldsymbol{S}_x(f) = \boldsymbol{G}(f)\boldsymbol{G}^H(f)$, where

$$\boldsymbol{G}(f) \triangleq \sum_\ell \boldsymbol{G}_\ell e^{-j2\pi f T_s \ell} \quad (7)$$

[1]The detailed derivation of (5) is skipped due to space constraints.

is the precoder transfer function. Hence, (5) becomes

$$S_s(f) = \frac{|H_{\mathrm{I}}(f)|^2}{LT_s} \left\| \boldsymbol{G}^H(Lf) \boldsymbol{\phi}(f) \right\|^2. \quad (8)$$

For a real-valued nonnegative weighting function $W(f)$, let $\widetilde{W}(f) \triangleq W(f) \frac{|H_{\mathrm{I}}(f)|^2}{LT_s}$. Then, the weighted power of $s(t)$ is

$$\begin{aligned} P_{\mathrm{W}} &= \int_{-\infty}^{\infty} W(f) S_s(f) df \\ &= \mathrm{tr} \int_{-\infty}^{\infty} \widetilde{W}(f) \boldsymbol{G}^H(Lf) \boldsymbol{\phi}(f) \boldsymbol{\phi}^H(f) \boldsymbol{G}(Lf) df \\ &= \mathrm{tr} \sum_\ell \sum_{\ell'} \boldsymbol{G}_{\ell'}^H \boldsymbol{\Phi}[\ell - \ell'] \boldsymbol{G}_\ell, \end{aligned} \quad (9)$$

where we have introduced the $K \times K$ matrices

$$\boldsymbol{\Phi}[b] \triangleq \int_{-\infty}^{\infty} \widetilde{W}(f) \boldsymbol{\phi}(f) \boldsymbol{\phi}^H(f) e^{-j2\pi L f T_s b} df. \quad (10)$$

Thus, (9) gives the weighted power P_{W} as a quadratic function of the precoder impulse response coefficients $\boldsymbol{G}_\ell$. More explicitly, and assuming an FIR precoder, let $\boldsymbol{G}_\ell = \boldsymbol{0}$ for $\ell < -\ell_1$ and $\ell > \ell_2$, with $-\ell_1 \leq 0 \leq \ell_2$. Let $\ell_0 = \ell_1 + \ell_2$ be the precoder order, and introduce the matrices

$$\boldsymbol{G} \triangleq \begin{bmatrix} \boldsymbol{G}_{-\ell_1}^H & \cdots & \boldsymbol{G}_0^H & \cdots & \boldsymbol{G}_{\ell_2}^H \end{bmatrix}^H, \quad (11)$$

$$\boldsymbol{\Phi} \triangleq \begin{bmatrix} \boldsymbol{\Phi}[0] & \boldsymbol{\Phi}[1] & \cdots & \boldsymbol{\Phi}[\ell_0] \\ \boldsymbol{\Phi}^H[1] & \boldsymbol{\Phi}[0] & \cdots & \boldsymbol{\Phi}[\ell_0 - 1] \\ \vdots & \vdots & \ddots & \vdots \\ \boldsymbol{\Phi}^H[\ell_0] & \boldsymbol{\Phi}^H[\ell_0 - 1] & \cdots & \boldsymbol{\Phi}[0] \end{bmatrix}. \quad (12)$$

Note that $\boldsymbol{\Phi}$ is block-Toeplitz and Hermitian. Then (9) can be rewritten as

$$P_{\mathrm{W}} = \mathrm{tr}\left\{ \boldsymbol{G}^H \boldsymbol{\Phi} \boldsymbol{G} \right\}. \quad (13)$$

3. PROPOSED MEMORY AIC PRECODER

In AIC, the set of active subcarriers is split between data and cancellation subcarriers. Thus, the data vector $\boldsymbol{d}_m$ is directly mapped to D of the K active subcarriers, whereas the remaining $K - D$ subcarriers are used for cancellation. Let $\boldsymbol{S} \in \mathbb{C}^{K \times D}$ comprise the D columns of the identity matrix $\boldsymbol{I}_K$ corresponding to the indices of the active subcarriers to which the data is directly mapped, and let $\boldsymbol{T} \in \mathbb{C}^{K \times K-D}$ comprise the remaining $K - D$ columns of $\boldsymbol{I}_K$. The impulse response of the memory AIC precoder must be given by

$$\boldsymbol{G}_0 = \alpha \boldsymbol{S} + \boldsymbol{T}\boldsymbol{Q}_0, \quad \boldsymbol{G}_\ell = \boldsymbol{T}\boldsymbol{Q}_\ell \text{ for } \ell \neq 0, \quad (14)$$

where $\alpha > 0$ controls the power allocation between data and cancellation subcarriers [13] , and $\boldsymbol{Q}_\ell$ are $K-D \times D$ matrices. Therefore, the precoded vector in (6) becomes

$$\boldsymbol{x}_m = \sum_\ell \boldsymbol{G}_\ell \boldsymbol{d}_{m-\ell} = \alpha \boldsymbol{S} \boldsymbol{d}_m + \boldsymbol{T} \sum_{\ell \neq 0} \boldsymbol{Q}_\ell \boldsymbol{d}_{m-\ell}. \quad (15)$$

Since $\boldsymbol{S}^H\boldsymbol{S} = \boldsymbol{I}_D$ and $\boldsymbol{S}^H\boldsymbol{T} = \boldsymbol{0}$, it is clear that $\boldsymbol{S}^H\boldsymbol{x}_m = \alpha\boldsymbol{d}_m$, so that $\boldsymbol{d}_m$ can be recovered from $\boldsymbol{x}_m$ by discarding the cancellation subcarriers.

The goal is to pick $\{\boldsymbol{Q}_\ell\}$ to minimize OBR for a given transmit power. OBR is computed via (9) by choosing a weighting function such that $W(f) > 0$ over the OBR region $\mathcal{B}$, and $W(f) = 0$ outside $\mathcal{B}$. Note, $\mathcal{B}$ may include parts within the passband of data subcarriers, e.g., to protect narrowband transmissions from other users in a dynamic spectrum sharing (DSS) setting. Also, cancellation subcarriers may be located inside and/or outside $\mathcal{B}$. The choice of values of $W(f)$ over $\mathcal{B}$ allows to emphasize OBR reduction in certain subbands over others. The problem can be stated as

$$\min_{\{\boldsymbol{Q}_\ell\}} P_{\mathrm{W}} \qquad \text{s. to} \qquad P_{\mathrm{T}} \le P_{\max}, \tag{16}$$

where P_{W} is given by (9), $P_{\mathrm{T}} = \int_{-\infty}^{\infty} S_s(f)df$ is the total transmit power, and $P_{\max}$ is the available power. Note that $P_{\mathrm{T}} = \mathrm{tr}\{\boldsymbol{G}^H\boldsymbol{\Phi}_{\mathrm{T}}\boldsymbol{G}\}$, where $\boldsymbol{\Phi}_{\mathrm{T}}$ is obtained analogously to (12) and (10), but for a weighting function $W(f) = 1\ \forall f$. The available power is set to the transmit power of an unprecoded system for which $\boldsymbol{x}_m = \boldsymbol{S}\boldsymbol{d}_m$, so that $P_{\max} = \mathrm{tr}\{\boldsymbol{S}^H\boldsymbol{\Phi}_{\mathrm{T}}\boldsymbol{S}\}$; in this way, we must set $\alpha < 1$ to allocate some power to cancellation subcarriers.

For an FIR AIC precoder as in (11), $\boldsymbol{G}$ can be written as

$$\boldsymbol{G} = \alpha\widetilde{\boldsymbol{S}} + \widetilde{\boldsymbol{T}}\boldsymbol{Q}, \tag{17}$$

where $\widetilde{\boldsymbol{T}} = \boldsymbol{I}_{\ell_0} \otimes \boldsymbol{T}$ with '$\otimes$' the Kronecker product, and

$$\widetilde{\boldsymbol{S}} = \left[\ \boldsymbol{0}^H_{\ell_1 K\times D} \quad \boldsymbol{S}^H \quad \boldsymbol{0}^H_{\ell_2 K\times D}\ \right]^H, \tag{18}$$

$$\boldsymbol{Q} = \left[\ \boldsymbol{Q}^H_{-\ell_1} \quad \cdots \quad \boldsymbol{Q}^H_0 \quad \cdots \quad \boldsymbol{Q}^H_{\ell_2}\ \right]^H. \tag{19}$$

Hence, the optimization problem (16) is a Least Squares (LS) problem with a Quadratic Inequality constraint (LSQI):

$$\min_{\boldsymbol{Q}} \mathrm{tr}\{(\alpha\widetilde{\boldsymbol{S}} + \widetilde{\boldsymbol{T}}\boldsymbol{Q})^H\boldsymbol{\Phi}(\alpha\widetilde{\boldsymbol{S}} + \widetilde{\boldsymbol{T}}\boldsymbol{Q})\}$$
$$\text{s. to} \quad \mathrm{tr}\{(\alpha\widetilde{\boldsymbol{S}} + \widetilde{\boldsymbol{T}}\boldsymbol{Q})^H\boldsymbol{\Phi}_{\mathrm{T}}(\alpha\widetilde{\boldsymbol{S}} + \widetilde{\boldsymbol{T}}\boldsymbol{Q})\} \le P_{\max}. \tag{20}$$

To solve (20), consider first the LS problem obtained by neglecting the constraint in (20), whose solution is given by

$$\boldsymbol{Q}_{\mathrm{LS}} = -\alpha\left(\widetilde{\boldsymbol{T}}^H\boldsymbol{\Phi}\widetilde{\boldsymbol{T}}\right)^{-1}\left(\widetilde{\boldsymbol{T}}^H\boldsymbol{\Phi}\widetilde{\boldsymbol{S}}\right). \tag{21}$$

If $P_{\mathrm{LS}} \triangleq \mathrm{tr}\{(\alpha\widetilde{\boldsymbol{S}} + \widetilde{\boldsymbol{T}}\boldsymbol{Q}_{\mathrm{LS}})^H\boldsymbol{\Phi}_{\mathrm{T}}(\alpha\widetilde{\boldsymbol{S}} + \widetilde{\boldsymbol{T}}\boldsymbol{Q}_{\mathrm{LS}})\} \le P_{\max}$, then it is clear that (21) is the solution to problem (20). On the other hand, if $P_{\mathrm{LS}} \ge P_{\max}$ (the usual case) then (21) is not feasible, and at the solution of (20) the constraint must hold with equality. The constrained solution is found to be

$$\boldsymbol{Q} = -\alpha\left[\widetilde{\boldsymbol{T}}^H(\boldsymbol{\Phi} + \lambda\boldsymbol{\Phi}_{\mathrm{T}})\widetilde{\boldsymbol{T}}\right]^{-1}\left[\widetilde{\boldsymbol{T}}^H(\boldsymbol{\Phi} + \lambda\boldsymbol{\Phi}_{\mathrm{T}})\widetilde{\boldsymbol{S}}\right]. \tag{22}$$

The value of the Lagrange multiplier λ can be obtained by substituting (22) in the power constraint (with equality) in (20); with the help of the generalized singular value decomposition (GSVD), a nonlinear equation for λ is obtained, which can be numerically solved easily [13], [17, Sec. 12.1.1].

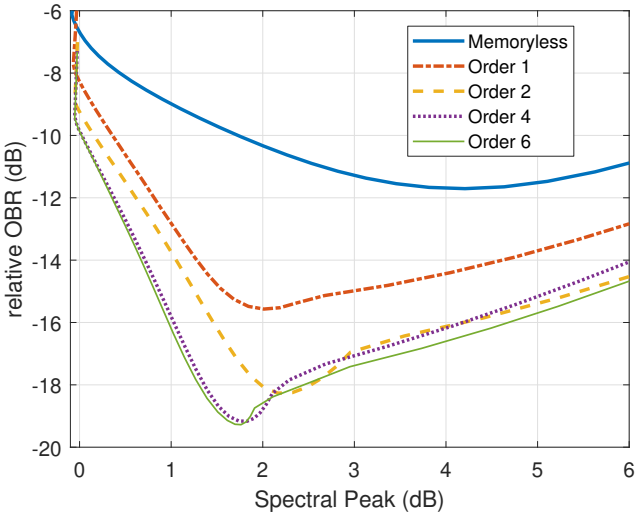

Fig. 1. OBR achieved with AIC precoders (relative to that of the unprecoded system) as a function of spectral overshoot. $D = 53$ data subcarriers.

4. RESULTS AND DISCUSSION

Consider a CP-OFDM scenario with IFFT size $N = 128$ and CP length $P = N/16$. The interpolation filter is taken as an ideal lowpass filter with $H_{\mathrm{I}}(f) = 1$ for $|f| \le \frac{1}{2T_s}$ and zero otherwise. Transmission is intended in the passband $|f| \le \frac{1}{4T_s} + \frac{\Delta f}{2}$, in which a maximum of $\frac{N}{2} + 1 = 65$ subcarriers can be accommodated; thus, $D \le 65$. The OBR is to be minimized over the region

$$\mathcal{B} = \left\{ f \;\middle|\; \frac{1}{4T_s} + \frac{\Delta f}{2} \le |f| \le \frac{1}{2T_s} \right\}, \tag{23}$$

with $W(f) = 1$ for $f \in \mathcal{B}$, and zero elsewhere. All $K = N$ subcarriers are active (thus including those in $\mathcal{B}$), so that the number of cancellation subcarriers is $N - D$. Data subcarriers are located symmetrically about the carrier frequency.

4.1. Effect of the parameter α

The value of α is related to the power allocation between cancellation and data subcarriers. The power allocated to the latter is $\alpha^2 P_{\max}$, so that there is an SNR penalty of $20\log_{10}\alpha$ dB at the receiver with respect to the unprecoded system. As α approaches 1, there is less power available to cancellation subcarriers, so that OBR reduction will suffer. On the other hand, decreasing α improves OBR reduction, but cancellation subcarriers located outside $\mathcal{B}$ will tend to produce large peaks in the PSD. This spectral overshoot is undesirable in practice, because spectral emission masks place upper bounds on the PSD relative to its maximum value. Hence, a tradeoff must be found between OBR performance and spectral overshoot. To illustrate this, consider the setting described above, with

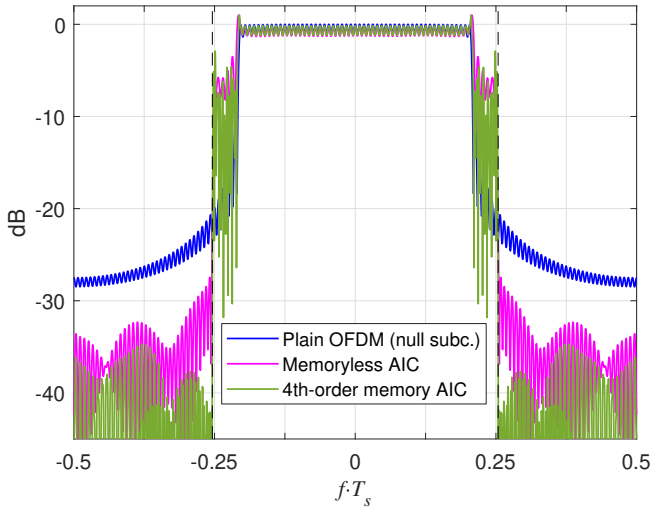

Fig. 2. PSDs for 1-dB spectral overshoot. $D = 53$ data subcarriers. Dashed vertical lines mark the OBR region $\mathcal{B}$.

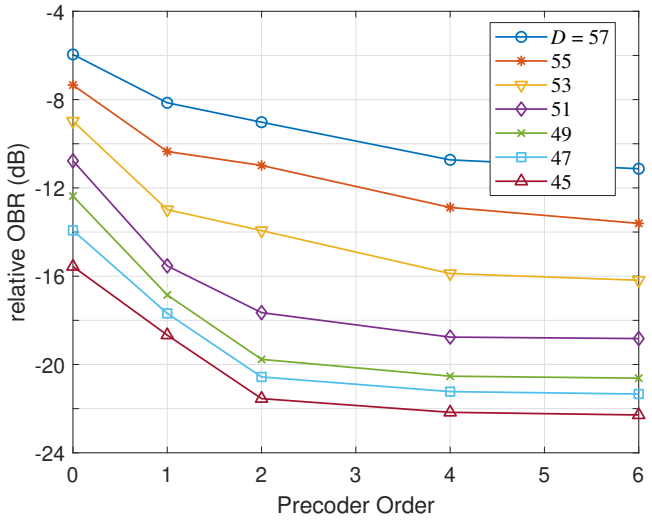

Fig. 3. OBR (relative to that of the unprecoded system) with memory AIC precoders of different orders, and for different number of data subcarriers D. Spectral overshoot is kept at 1 dB in all cases.

data transmission making use of the central $D = 53$ subcarriers for an efficiency of $\frac{53}{65} = 81.5\%$. The standard memoryless AIC precoder is consider, together with the proposed FIR designs of first, second, fourth and sixth order, for which $(\ell_1, \ell_2) = (0,1)$, $(1,1)$, $(2,2)$ and $(3,3)$ respectively. For each of them, the OBR and spectral peak size are recorded for each value of $\alpha \in [0.8, 1]$, and the resulting curves are shown in Fig. 1. For α close to 1 (left side of the figure), there is no spectral overshoot, but OBR reduction is poor. As α is decreased and the spectral peak becomes larger, an improvement in OBR performance is observed; however, beyond some point, OBR starts to degrade. For small spectral overshoot, which is of practical interest, it is clear that a much better tradeoff can be achieved with memory AIC precoders, since their corresponding curves in Fig. 1 are much steeper than that of the memoryless AIC precoder.

4.2. Benefits of memory precoding

Fig. 2 shows the PSD obtained in the setting above, and computed via (5), again for $D = 53$ data subcarriers, and for three cases: an unprecoded system (only D subcarriers active), memoryless AIC, and the proposed AIC design of order 4 ($\ell_1 = \ell_2 = 2$). For both AIC schemes α was set for a 1-dB spectral peak. The memory-based design clearly improves upon the standard memoryless AIC scheme; in terms of OBR reduction the improvement is ≈ 7 dB in this example.

For a given value of the maximum spectral peak, the only way to further reduce OBR with the memoryless AIC scheme is to increase the number of cancellation subcarriers, at the expense of reducing the spectral efficiency of the system. As shown in Fig. 2, the introduction of memory provides an alternative, by which OBR performance can be improved without degrading spectral efficiency.

This fact is further illustrated in Fig. 3, which represents the OBR performance in this setting as a function of the order of the memory AIC precoder (zeroth-order corresponds to the standard memoryless design), and for different values of the number of data subcarriers D, when the spectral peak is limited to 1 dB. It is seen that for a given precoder order, performance improves as the number of cancellation subcarriers increases, as expected. In addition, for a given value of D, performance also improves as the precoder order is increased. The obtained gains eventually saturate, since the contribution of symbols far away from the current one becomes less significant; therefore, there seems to be little incentive to consider memory precoders of order larger than four. This trend has also been observed in other settings in all experiments conducted. Fig. 3 also shows the spectral efficiency savings that can be obtained by introducing memory in the AIC precoder: for example, the performance of the memoryless precoder with $D = 47$ (efficiency $\frac{47}{65} = 72.3\%$) can be achieved either with a second-order design and $D = 53$ (81.5%) or with a sixth-order design and $D = 55$ (84.6%). Analogously, the performance of the memoryless precoder with $D = 45$ (69.2%) can be achieved with a first-order design and $D = 51$ (78.4%) or with a fourth-order design and $D = 53$ (81.5%).

4.3. Complexity and latency

The design of the AIC precoder coefficients is data-independent, and thus it can be performed offline; although in DSS scenarios in which spectral occupancy by other users changes dynamically, it may become necessary to recompute the precoders on the fly. Computation of the coefficients via (22)

is dominated by the GSVD of two matrices of size $\ell_0(K-D)\times\ell_0(K-D)$ needed to find the Lagrange multiplier, and by solving the linear system of equations (22) whose matrix also has this size. Thus, offline computational complexity is $O(\ell_0^3(K-D)^3)$. On the other hand, online operation is determined by (15), with complexity $O(\ell_0(K-D)D)$; this cost is incurred at the transmitter side. Therefore, the benefits of introducing memory in AIC precoders come at the price of increased computational complexity, both offline (cubic in the precoder order ℓ_0) and online (linear in ℓ_0).

In addition, the use of an FIR memory precoder (11) introduces a latency of ℓ_1 OFDM symbols in the transmission, since the precoding operation is necessarily causal. In general, for a fixed precoder order $\ell_0 = \ell_1 + \ell_2$ and a given spectral peak value, choosing $\ell_1 = \ell_2 = \frac{\ell_0}{2}$ provides slightly better OBR than $\ell_1 = 0$, $\ell_2 = \ell_0$, but the latter choice may be preferable in latency-critical scenarios.

5. CONCLUSION

Active interference cancellation is an appealing technique to reduce out-of-band radiation whenever transparency at the receiver is required, but standard memoryless designs must pay a steep price in spectral efficiency. The introduction of memory alleviates this tradeoff at the cost of additional computational complexity at the transmitter. The proposed design allows to specify the frequency region of interest and to weight the influence of out-of-band emission. As it has been assumed that the location of cancellation subcarriers is fixed *a priori,* the optimization of such locations following the steps of [13] seems an interesting approach to further boost performance.

6. REFERENCES

[1] Group Radio Access Network, "TS38.211: NR; Physical channels and modulation (Release 15)," `https://portal.3gpp.org/desktopmodules/Specifications/SpecificationDetails.aspx?specificationId=3213`, Mar. 2018.

[2] M. Faulkner, "The effect of filtering on the performance of OFDM systems," *IEEE Trans. Veh. Technol.*, vol. 49, no. 5, pp. 1877–1884, 2000.

[3] X. Huang, J. A. Zhang, and Y. J. Guo, "Out-of-band emission reduction and a unified framework for precoded OFDM," *IEEE Commun. Mag.*, vol. 53, no. 6, pp. 151–159, Jun. 2015.

[4] M.-F. Tang and B. Su, "Joint window and filter optimization for new waveforms in multicarrier systems," *EURASIP J. Adv. Signal Process.*, vol. 2018, no. 1, pp. 63–82, Oct. 2018.

[5] C.-D. Chung, "Spectrally precoded OFDM," *IEEE Trans. Commun.*, vol. 54, pp. 2173–2185, Dec. 2006.

[6] J. van de Beek, "Sculpting the multicarrier spectrum: a novel projection precoder," *IEEE Commun. Lett.*, vol. 13, no. 12, pp. 881–883, Dec. 2009.

[7] M. Ma, X. Huang, B. Jiao, and Y. J. Guo, "Optimal orthogonal precoding for power leakage suppression in DFT-based systems," *IEEE Trans. Commun.*, vol. 59, no. 3, pp. 844–853, Mar. 2011.

[8] K. Hussain, A. Lojo, and R. López-Valcarce, "Flexible spectral precoding for sidelobe suppression in OFDM systems," in *IEEE Int. Conf. Acoust., Speech, Signal Process. (ICASSP)*, May 2019, pp. 4789–4793.

[9] A. Zaidi, F. Athley, J. Medbo, U. Gustavsson, G. Durisi, and X. Chen, *5G Physical Layer: Principles, Models and Technology Components*, Academic Press, London, UK, 2018.

[10] S. Brandes, I. Cosovic, and M. Schnell, "Reduction of out-of-band radiation in OFDM systems by insertion of cancellation carriers," *IEEE Commun. Lett.*, vol. 10, no. 6, pp. 420–422, Jun. 2006.

[11] H. Yamaguchi, "Active interference cancellation technique for MB-OFDM cognitive radio," in *34th Eur. Microwave Conf.,*, 2004, vol. 2, pp. 1105–1108.

[12] S. Huang and C. Hwang, "Improvement of active interference cancellation: avoidance technique for OFDM cognitive radio," *IEEE Trans. Wireless Commun.*, vol. 8, no. 12, pp. 5928–5937, 2009.

[13] J. F. Schmidt, S. Costas-Sanz, and R. López-Valcarce, "Choose your subcarriers wisely: Active interference cancellation for cognitive OFDM," *IEEE J. Emerg. Sel. Topics Circuits Syst.*, vol. 3, no. 4, pp. 615–625, Dec. 2013.

[14] J. F. Schmidt, D. Romero, and R. López-Valcarce, "Active interference cancellation for OFDM spectrum sculpting: Linear processing is optimal," *IEEE Commun. Lett.*, vol. 18, no. 9, pp. 1543–1546, Sep. 2014.

[15] J. Van De Beek and F. Berggren, "Out-of-band power suppression in OFDM," *IEEE Commun. Lett.*, vol. 12, no. 9, pp. 609–611, 2008.

[16] J. Haber-Kucharsk, E. Haj Mirza Alian, and P. Mitran, "On the reserved sub-carrier approach to achieving N-continuity for side-lobe reduction in OFDM," in *13th Can. Workshop Inf. Theory (CWIT)*, 2013, pp. 209–213.

[17] G. H. Golub and C. F. Van Loan, *Matrix Computations (3rd Ed.)*, Johns Hopkins University Press, Baltimore, MD, USA, 1996.